



HAL
open science

Biogeochemical impact of tropical instability waves in the equatorial Pacific

Thomas Gorgues, Christophe E. Menkès, Olivier Aumont, Jérôme Vialard, Yves Dandonneau, Laurent Bopp

► **To cite this version:**

Thomas Gorgues, Christophe E. Menkès, Olivier Aumont, Jérôme Vialard, Yves Dandonneau, et al.. Biogeochemical impact of tropical instability waves in the equatorial Pacific. *Geophysical Research Letters*, 2005, 32, pp.L24615. 10.1029/2005GL024110 . hal-00122343

HAL Id: hal-00122343

<https://hal.science/hal-00122343>

Submitted on 26 Mar 2007

HAL is a multi-disciplinary open access archive for the deposit and dissemination of scientific research documents, whether they are published or not. The documents may come from teaching and research institutions in France or abroad, or from public or private research centers.

L'archive ouverte pluridisciplinaire **HAL**, est destinée au dépôt et à la diffusion de documents scientifiques de niveau recherche, publiés ou non, émanant des établissements d'enseignement et de recherche français ou étrangers, des laboratoires publics ou privés.

Biogeochemical impact of Tropical Instability Waves in the Equatorial Pacific

T. Gorgues (1), C. Menkes (1), O. Aumont (3), J. Vialard (1), Y. Dandonneau (1), L. Bopp (2)

(1) LOCEAN, Case 100, 4 place Jussieu, 75252 Paris, France.

(2) LSCE, CE Saclay, 91191 Gif sur Yvette, France.

(3) LOCEAN, Centre IRD de Bretagne, BP 70, 29280 Plouzané, France.

Abstract

Tropical Instability Waves (TIW) have been suggested to fertilize the equatorial Pacific in iron leading to enhanced ecosystem activity. Using a coupled dynamical–biogeochemical model, we show that contrary to this suggestion, TIWs induce a decrease of iron concentration by 20% at the equator and by about 3% over the “TIW box” [90°W–180, 5°N–5°S]. Chlorophyll decreases by 10% at the equator and 1% over the “TIW box”. This leads to a decrease of new production up to 10% at the equator (4% over the “TIW box”). TIW-induced horizontal advection brings more iron-depleted water to the equator than it exports iron-rich equatorial water to the north. Additional iron decrease is caused by TIW-induced iron vertical diffusion. These two mechanisms are partly counter balanced by a decrease of iron biological uptake, driven by weaker phytoplankton concentration, and to a lesser extent by TIW-induced iron vertical advection.

1. Introduction

From June to December, in the Pacific Ocean, meridional undulations in Sea Surface Temperature (hereafter SST) and chlorophyll front between cold and rich water from the equatorial upwelling and warm nutrient-depleted water from the north are observed from space [Legeckis 1977; Chavez et al., 1999; Chelton et al., 2000; Menkes et al., 2002; Strutton et al., 2001]. These features are referred to as Tropical Instability Waves (TIW). These oscillations have a longitudinal scale of 1000-1500km [Qiao & Weisberg, 1995] and are associated to anticyclonic Tropical Instability Vortices (hereafter TIV) (Figure 3F) [Flament et al., 1996; Kennan & Flament, 2000; Menkes et al., 2002]. They propagate westward at $30\text{-}60\text{ cm.s}^{-1}$ [Weidman et al., 1999]. Most of the energy of these TIWs are in the 20-40 day band [Weidman et al., 1999, Lyman et al., 2004].

TIV are three-dimensional structures with strong meridional and zonal current, but also with strong vertical currents ($10\text{ to }50\text{ m.day}^{-1}$) [Flament et al., 1996, Menkes et al., 2002] from the surface to the thermocline. Downwelling is found in the leading edge and upwelling in the trailing edge of TIVs (figure 3F). Locally, in convergence regions near the fronts, very high chlorophyll concentrations up to 2 mg.m^{-3} have been monitored from moorings [Strutton et al., 2001] and from space as a “line in the sea” [Yoder et al., 1994]. At a broader scale, satellite pictures also show clear meridional oscillations of the front separating equatorial rich water and oligotrophic water from the north [Chavez et al., 1999]. It has been hypothesised that these structures are the result of a complex balance between several processes including meridional advection, and upwelling of iron at TIV scale, that would allow for enhanced biomass [Strutton et al., 2001].

Thus this TIW-induced upwelling has been suggested to have a net fertilization effect on the climatology of the equatorial region [Murray et al., 1994; Yoder et al., 1994; Strutton et al., 2001; Menkes et al., 2002]. This hypothesis is difficult to investigate with data only. Numerical simulations can be used to investigate such aspects. In this paper, we use a biogeochemical model forced by realistic dynamical simulations to evaluate the impact of TIWs on the biogeochemical climatology of the equatorial Pacific.

2. Method

The dynamical model we use to force the biogeochemical model is the Ocean General Circulation Model, OPA [Madec et al, 1998], in a global configuration with a focus on the tropical Pacific. The model has a 2° zonal resolution, 31 levels and meridional resolution varies from 0.5° in the equatorial waveguide to 2° at the pole. Further description of this model can be found in Lengaigne et al., [2003]. The momentum forcing is from a combination of ERS1-2 and TAO (Tropical Atmosphere Ocean project) stresses as described in Lengaigne et al., [2003] over 1992-1998 period. Heat and water fluxes are from a daily climatology from the NCEP 1 (National Centers for Environmental Prediction) reanalyses [Kalnay et al., 1996].

The OPA outputs (the 3-D velocities u, v, w and vertical diffusion coefficient k) are used to force offline the PISCES biogeochemical model [Aumont et al., 2003]. PISCES attempts to reproduce the cycle of major nutrients (P, N, Si and Fe) with 2 phytoplankton, 2 zooplankton species and 2 sinking particles classes. Phytoplankton growth is limited by external concentration of iron, nitrate, silicate, ammonium, and phosphate. A constant Redfield ratio is used, except when a nutrient becomes limiting. In this case elemental ratios of silicate, iron, and chlorophyll are prognostically predicted based on external concentrations of limiting nutrients. This choice is justified by the fact that in observations this ratio is highly variable. For example Fe/C ratio can vary by an order of magnitude [Sunda and Hutsman, 1997].

We base the analysis on two biogeochemical simulations. The first simulation (FULL) is the reference simulation where 5-day dynamical fields are used to force offline the biogeochemical model over the 1992-1998 time period. In a second simulation (NOTIW), we time-average every 7 consecutive dynamical outputs to obtain dynamical forcings representing 35-day means. The purpose of this procedure is to filter out the TIW variability in the eastern Pacific dynamics, while keeping a same dynamical mean state. With identical initial conditions than in FULL, we force PISCES offline with these filtered fields over the same period. While we are aware that we filter out also some of the variability of other phenomena such as intraseasonal Kelvin waves, the dominant variability in the eastern Pacific at monthly time scales takes the form of TIWs [Vialard et al., 2001; Menkes et al., 2005].

The comparisons between the biogeochemical fields of the two simulations, allow inferring the role of TIWs on mean biogeochemical budgets.

3. Model Validation

In this section, we compare the FULL simulation to the data. The model SST is too warm by about 0.5°C in our simulation (not shown), but the main patterns match the observations. In the eastern Pacific, TIW is the dominant variability at monthly time scale and has wavelengths, period and propagation features close to those in observations (not shown). More validation of the statistics of the TIWs, of temperature structures and surface current comparisons can be found in Vialard et al., [2002]; Lengaigne et al., [2003]; and Menkes et al., [2005].

The FULL chlorophyll mean over 1992-1998 is compared against the 1998-2004 SeaWifs mean chlorophyll (Figure 1A-B). Despite too weak coastal upwelling signals and too depleted gyres and warm pool, the model chlorophyll gives realistic patterns, especially in the central-eastern equatorial region and are comparable to other model chlorophyll [Christian et al., 2002; Wang et al., 2005]. As, in the equatorial Pacific iron is known to be a limiting nutrient, it is crucial to simulate iron concentration adequately. In Figure 1C, model iron profiles are compared to observations along 140°W in the [3S°-9°N] band where data was available [Coale et al., 1996] and where TIWs are strong. This modelled mean profile shows good correspondence in terms of values and gradients, especially at the ferricline level.

Finally, table 1 gives a comparison of our model to other published new production estimates from *in situ* measurements and other model data for the eastern equatorial region. Our model estimate is in the range of the other data which, together with previous validation, gives us confidence in the main processes at work in the model in the central-eastern Pacific

4. Discussion

We limit our discussion to the [160°W-80°W/5°S-5°N] region in which TIWs are most active. Iron being the limiting nutrient for phytoplankton growth in our region; we will focus the discussion on iron to understand the main chlorophyll and new production patterns. All fields are averaged over the euphotic layer (defined as 0.1% light level).

It has been hypothesized that TIWs could contribute to enhance the upper ocean fertilization by promoting locally iron upwelling [Foley et al, 1997]. From NOTIW experiment, it would rather seem that the effect of TIWs is to decrease iron concentration very near the equator by up to 20% (Figure 2A-B). Over the “TIW box”, this decrease is about 3%. Time series (not shown), show that this decrease is systematically observed every year and concentrated during active phases of TIWs during summer and fall. To understand this, we turn to the iron concentration balance in the model:

$$\partial_t Fe = \underbrace{-u\partial_x Fe - v\partial_y Fe - w\partial_z Fe}_a + \underbrace{D_l(Fe)}_c + \underbrace{\partial_z(k\partial_z Fe)}_d + \underbrace{SMS}_e \quad (1)$$

Iron variability is the results of a balance between horizontal advection (term a), vertical advection (term b), lateral diffusion (term c, that can be neglected in comparison with other terms), vertical diffusion (term d) and the “SMS” term (term e) that represents the sources minus sinks in the biogeochemical model. That term includes processes like iron uptake by phytoplankton, loss by sedimentation etc. which are detailed in Aumont et al., [2005]. For the purpose of the present paper, we consider this term as the net effect of biogeochemistry. To understand the average iron concentration difference between FULL and NOTIW, we can derive from (1) the following equation:

$$\overline{Fe_F} - \overline{Fe_N} = \frac{1}{(t_f - t_0)} \int_{t_0}^{t_f} (\int_{t_0}^{t_f} (\partial_u Fe_F - \partial_u Fe_N) du) dt \quad (2)$$

where Fe_F and Fe_N are the iron concentration of FULL and NOTIW, respectively and the overbar denotes the average between $t_0=01/01/1992$ and $t_f=31/12/1998$. The left term of equation (2) is shown on figure 2B. Replacing the right hand side of equation (2) by the individual processes of equation (1), allows examining the contribution of advection, diffusion and biological processes leading to the differences in Figure 2B.

Figure 3A shows the contribution of horizontal advection. TIWs act to remove up to 1.5 nM of iron in a narrow equatorial band, essentially via meridional advection (not shown). The northward branch of the TIV carries equatorial iron-rich water northward, while the southward branch brings poor water from the north to the equator,

resulting in a net iron loss by TIW-induced lateral advection near the equator. It is worth pointing out that this value is two orders of magnitude greater than concentration differences in Figure 2B. Other processes in equation (1) must compensate this term. Figure 3C shows that modification of the effect of TIW-vertical diffusion of iron is also to reduce concentrations at the equator with values smaller than those induced by horizontal advection (except near the South American coast). We observe the same kind of decreased iron concentration in the leading edge of TIWs, near 4°N (Figure 3E).

In contrast, the TIW impact on vertical advection (Figure 3B) and biological activity (Figure 3D) is to increase iron in the euphotic layer. These two terms compensate the loss induced by TIWs via horizontal advection and vertical diffusion. TIW related vertical advection brings iron in the euphotic layer in areas of TIW-induced upwelling (Figure 3F), but TIW-induced vertical advection of iron is always about 5 times smaller than horizontal advection (Figure 3A-B). This suggests that TIWs do not act as an iron fertilizer via their induced upwelling. This also can be inferred at TIW scale where phytoplankton rich areas are found in the downwelling areas and not in the upwelling areas (Figure 3E-F).

The chlorophyll patterns show similar behaviours (Figure 2D) to those of iron. Because TIWs tend to reduce iron in the euphotic zone, they induce a decrease in phytoplankton and chlorophyll concentrations near the equator (up to 10%, and 1% over “TIW box”) (Figures 2C and D). The decrease of biological uptake associated to the weaker concentration of chlorophyll is a major contributor to the iron balance (Figure 3D) with values of the same order as those of horizontal advection (Figure 3A) at the equator and values cancelling out those from vertical diffusion at 4°N (Figure 3C). This results in positive values of Figure 3D as the biological sink removes less iron.

Figure 3 shows that individual processes contributing to the iron balance are strongly changed by removing TIWs variability. The individual terms in the right hand side of equation 2 are two orders of magnitude larger than the net iron concentration change. This suggests that despite the strong dynamical change associated to the suppression of TIWs, there is a strong feedback that maintains the biogeochemical concentration in a tight range. Biogeochemical feedbacks may thus act to compensate the TIWs modification induced by the dynamical terms.

Finally, a good measure of the integrated effect of TIWs on ecosystem activity may be seen in new production patterns (Figure 2E). As expected from other Figure 2 panels, the action of TIWs is limited to a narrow equatorial

strip as for iron. TIWs tend to reduce new production (and primary production) by up to 10% (Figure 2F) and only 4% over the “TIW box”.

5. Conclusion

In this study, we have used the PISCES model [Aumont et al., 2005], forced by outputs from the OPA ocean general circulation model, to investigate the effect of TIWs on the long-term average biogeochemical conditions in the equatorial Pacific. The main effect of TIWs over the 1992-1998 period is to reduce iron concentration at the equator up to 20% and by about 3% over the “TIW box”. This results from a complex balance between several processes. TIWs reduce iron concentration in the equatorial strip via horizontal advection (primarily by meridional advection) and, to a lesser extent, via eddy vertical diffusion. These effects are partially compensated by iron input due to TIW-induced vertical advection and reduced phytoplankton uptake. TIW-vertical input of iron is small (~20%) compared to TIW-induced lateral advection of iron-poor water. Since iron is limiting biogeochemical growth in this region, TIWs decrease chlorophyll concentration and new production by about 10% in the equator and only by 1-4% over the “TIW box”.

These results are contrary to hypotheses drawn from many observation papers [Murray et al., 1994; Yoder et al., 1994; Strutton et al., 2001; Menkes et al., 2002] where it was suggested that TIW variability could have a net fertilization effect via TIW-induced upwelling in a narrow equatorial strip. There is no doubt however that TIWs indeed strongly modulate the biogeochemical distribution in the equatorial rich region [Chavez et al., 1999; Strutton et al., 2001; Menkes et al., 2002]. Satellite and in situ data show that TIWs have two effects: on the one hand they displace equatorial rich chlorophyll regions to the north of the equator in response to northward advection, but they also bring oligotrophic water from the north. Our results suggest that the southward advection of biologically poor water is the main process leading to iron reduction at the equator. In addition, we found that TIWs induce an additional reduction of iron input via eddy vertical diffusion. Finally, our results suggest that TIWs are not a major contributor to the net mean new production as they contribute to decrease it for a maximum of 10% at the equator.

There is however no contradiction with the fact that dramatic increase of chlorophyll can be observed [Murray et al., 1993; Yoder et al., 1994; Strutton et al., 2001] at convergent areas (downwelling) induced by TIWs. This process of “lines in the sea” is probably linked to concentration of buoyant species in the convergence as suggested by Yoder et al., [1994] and similar to the one invoked in the “Hay Rake” mechanism on larger scales [Dandonneau et al., 2003] or on TIW scales [Dandonneau et al., 2005].

Suppressing TIWs result in large changes of the diffusion and advection terms in equation 1. The resulting change in biogeochemical concentrations, however, is two orders of magnitude smaller. This suggests that there are feedback terms, may be linked to biogeochemistry, that maintain the concentrations in a tight range.

Thus it is clear that even if TIWs do not have a major effect on mean ecosystem budget, the shape of the dynamics and ecosystem in the three dimensional Tropical instability Wave are still to be understood in the real ocean, which advocates for further modelling and observational studies.

References

- Aumont, O., et al. (2003), An ecosystem model of the global ocean including Fe, Si, P colimitations, *Global Biogeochem. Cycles*, 17(2), 1060, doi:10.1029/2001GB001745.
- Aumont, O., et al. (2005), Globalizing results from ocean in situ iron fertilization studies, submitted
- Chai, F., et al. (1996), Origin and maintenance of a high nitrate condition in the equatorial Pacific, *Deep-Sea Res. II*, 43, 1031-1064
- Chavez, F. P., et al. (1999), Biological and chemical response of the equatorial Pacific Ocean to the 1997– 98 El Niño, *Science*, 286, 2126–2131.
- Chavez, F. P., and R. T. Barber (1987), An estimate of new production in the equatorial Pacific, *Deep-Sea Res.*, 34, 1229-1243.
- Chelton, D. B., et al. (2000), Satellite microwave SST observations of transequatorial tropical instability waves, *Geophys. Res. Lett.*, 27(9), 1239–1242.
- Coale, K. H., et al. (1996), Control of community growth and export production by upwelled iron in the equatorial Pacific Ocean, *Nature*, 379, 621–624.

- Dandonneau, Y., et al. (2003), Oceanic Rossby Waves Acting As a "Hay Rake" for Ecosystem Floating By-Products, *Science*, 302, 1548-1551
- Dandonneau, Y., et al. (2005), Concentration of floating biogenic products in convergence zones, submitted
- Flament, P., et al. (1996), The three dimensional structure of an upper ocean vortex in the tropical Pacific, *Nature*, 382, 610–613.
- Foley, D. G., et al. (1997), Longwaves and primary productivity variations in the equatorial Pacific at 0°, 140°W, *Deep-Sea Res. II*, 44, 1801–1826,.
- Kalnay, E., et al. (1996), The NCEP/NCAR 40-Year Reanalysis Project, *Bull. Amer. Meteor. Soc.*, 77, 437–471.
- Kennan, S., and P. Flament (2000), Observations of a tropical instability vortex, *J. Phys. Oceanogr.*, 30, 2277–2301.
- Ku, T.L., et al. (1995), 228Ra-derived nutrient budgets in the upper equatorial Pacific and the role of “new” silicate in limiting productivity, *Deep-Sea Res. II*, 42, 479-497
- Weidman, P. D., et al. (1999), Analysis of Legeckis eddies in the near-equatorial Pacific, *J. of Geophysical Research.*, 104(C4), 7865-7888.
- Legeckis, R. (1977), Long waves in the eastern equatorial Pacific Ocean: A view from a geostationery satellite, *Science*, 197, 1179– 1181.
- Lengaigne, M., et al. (2003), Impact of isopycnal mixing on the tropical ocean circulation, *J. Geophys. Res.*, 108(C11), 3345, doi:10.1029/2002JC001704.
- Lyman, J. M., et al. (2004), Tropical Instability Waves as a Resonance between equatorial Rossby Waves, *J. of Physical Oceanography*, 35, 232-254.
- Madec, G., et al. (1998), OPA 8.1 Ocean General Circulation Model reference manual, *Notes du Pole de Modélisation de l'Institut Pierre-Simon Laplace*, 11, 91 pp. (Available from <http://www.lodyc.jussieu.fr/opa>).
- Menkes, C. E., et al. (2002), A whirling ecosystem in the equatorial Atlantic, *Geophys. Res. Lett.*, 29(11), 1553, doi:10.1029/2001GL014576.

Menkes, C. E., et al. (2005), A modelling study of the three-dimensional heat budget of Tropical Instability Waves in the Equatorial Pacific, *J. Phys. Oceanogr.*, in revision

Qiao, L., R. H. Weisberg (1995), Tropical instability wave kinematics: Observations from the Tropical Instability Wave Experiment, *J. Geophys. Res.*, *100(C5)*, 8677-8693.

Stoens, A., et al. (1999), The coupled physical-new production system in the equatorial Pacific during the 1992–1995 El Niño. *J. Geophys. Res.*, *104*, 3323–3339.

Strutton, P. G., et al. (2001), Enhanced chlorophyll associated with tropical instability waves in the equatorial Pacific, *Geophys. Res. Lett.*, *28*, 2005-2008.

Sunda, W. G., and S. A. Huntsman (1997), Interrelated influence of iron, light and cell size on marine phytoplankton growth, *Nature*, *390*, 389– 392.

Toggweiler, J.R., and S. Carson (1995), What are upwelling systems contributing to the ocean's carbon and nutrient budgets, In: *Upwelling in the ocean : Modern Process and Ancient Records*, C.P. Summerhayes, M.V. Angel, R.L. Smith, and B. Zeitzschel (eds), John Wiley & Sons Ltd, 337-360

Vialard, J., et al. (2001), A model study of oceanic mechanisms affecting equatorial Pacific sea surface temperature during the 1997–98 El Niño, *J. Phys. Oceanogr.*, *31*, 1649-1675

Vialard, J., et al. (2002), Sensitivity of Pacific Ocean Tropical Instability Waves to Initial Conditions, *J. Phys. Oceanogr.*, *33*, 105-121.

Yoder, J. A., et al. (1994), A line in the sea, *Nature*, *371*, 689– 692.

Figure captions

Figure 1: Chlorophyll surface concentration ($mg.m^{-3}$) for the FULL experiment (A) and for Seawifs data (B). Iron vertical profile (C) along 140°W, 3°S-9°N for FULL (shaded region) and for data (stars). The “TIW box” [90°W-180, 5°N-5°S] is represented in the first panel as a black box.

Figure 2: Average concentration in the euphotic zone in FULL for, iron (in nM) (A), chlorophyll (μM) (C) and new production ($mmolN.m^{-2}.day^{-1}$) (E). Differences (FULL-NOTIW) of concentrations for, iron (B), chlorophyll (D) and new production (E). Dashed lines represent negative contour.

Figure 3: Differences (FULL-NOTIW) averaged over the euphotic layer of iron 1992-1998 integrated trends (nM) from equation (1-2): A) horizontal advection, B) vertical advection, C) vertical diffusion, D) biological sources and sinks. The two other panels are snapshot of chlorophyll concentration (μM) with temperature contour (E) and snapshot of horizontal current drawn as vectors in $m.s^{-1}$, with vertical current colored in $m.day^{-1}$ (F). Negative values (blue) correspond to downwelling and upwelling (positive values) is in red.

Table 1: Integrated new production ($mmolN.m^{-2}.day^{-1}$) over $90^{\circ}W-180, 5^{\circ}N-5^{\circ}S$. Our model is in the range of previous studies.

Tables

Integrated New Production	
Chavez & Barber, 1987	2.7
Chai et al., 1996	2.3
Ku et al., 1995	2.5
Toggweiler & Carlson, 1995	3.3
Stoens et al, 1999	2.3
This study	3.0

Table 1: Integrated new production ($mmolN.m^{-2}.day^{-1}$) over $90^{\circ}W-180, 5^{\circ}N-5^{\circ}S$. Our model is in the range of previous studies

Figures

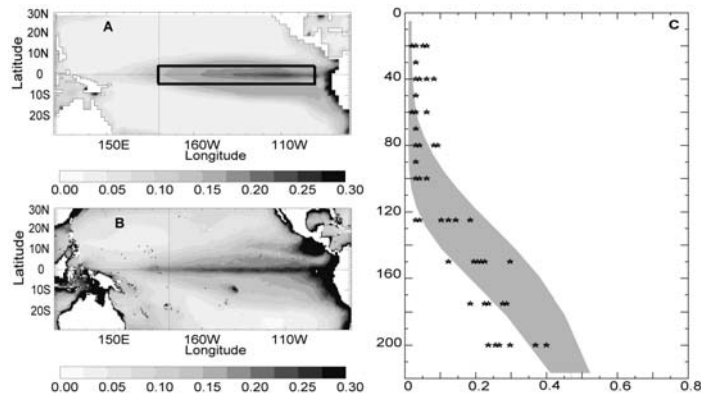


Figure 1: Chlorophyll surface concentration ($mg.m^{-3}$) for the FULL experiment (A) and for Seawifs data (B). Iron vertical profile (C) along $140^{\circ}W$, $3^{\circ}S$ - $9^{\circ}N$ for FULL (shaded region) and for data (stars). The “TIW box” [$90^{\circ}W$ - 180 , $5^{\circ}N$ - $5^{\circ}S$] is represented in the first panel as a black box.

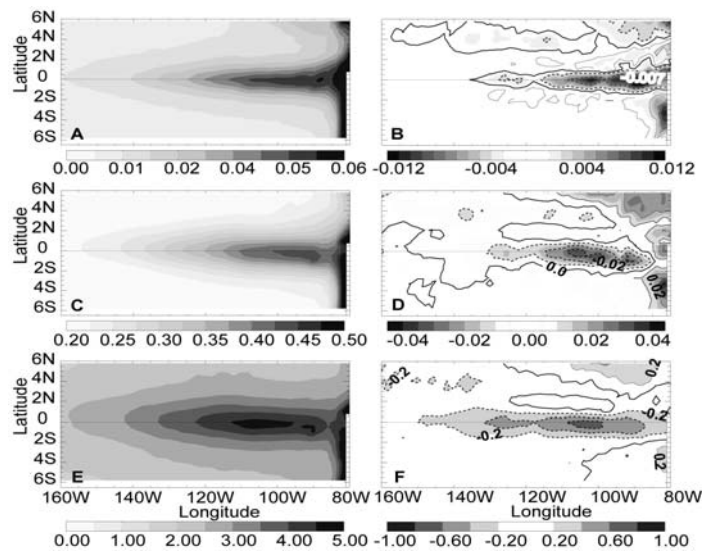


Figure 2: Average concentration in the euphotic zone in FULL for, iron (in nM) (A), chlorophyll (μM) (C) and new production ($mmolN.m^{-2}.day^{-1}$) (E). Differences (FULL-NOTIW) of concentrations for, iron (B), chlorophyll (D) and new production (E). Dashed lines represent negative contour.

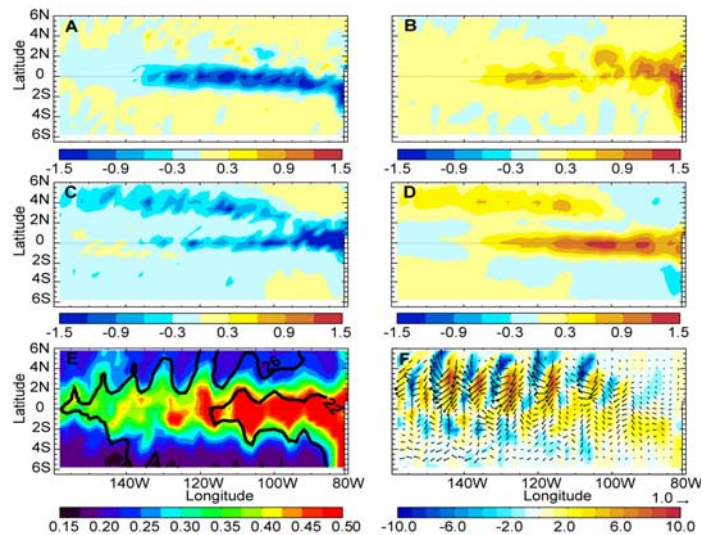


Figure 3: Differences (FULL-NOTIW) averaged over the euphotic layer of iron 1992-1998 integrated trends (nM) from equation (1-2): A) horizontal advection, B) vertical advection, C) vertical diffusion, D) biological sources and sinks. The two other panels are snapshot of chlorophyll concentration (μM) with temperature contour (E) and snapshot of horizontal current drawn as vectors in $m.s^{-1}$, with vertical current colored in $m.day^{-1}$ (F). Negative values (blue) correspond to downwelling and upwelling (positive values) is in red.